Enhanced photoabsorption efficiency of incomplete nanoshells

Murugesan Venkatapathi,[1,*] Sudipta G. Dastidar,[2] P. Bharath,[2] Arindam Roy,[2] and Anupam Ghosh[1]

[1]*Computational Photonics Laboratory, SERC, Indian Institute of Science, Bangalore 560012, India*

[2]*Unilever Research & Development, Whitefield, Bangalore 560066, India*

**Corresponding author: murugesh@serc.iisc.ernet.in*

Received May 29, 2013; revised July 8, 2013; accepted July 24, 2013;
posted July 25, 2013 (Doc. ID 191383); published August 22, 2013

The rather low scattering or extinction efficiency of small nanoparticles, metallic and otherwise, is significantly enhanced when they are adsorbed on a larger core particle. But the photoabsorption by particles with varying surface area fractions on a larger core particle is found to be limited by saturation. It is found that the core-shell particle can have a lower absorption efficiency than a dielectric core with its surface partially nucleated with absorbing particles—an "incomplete nanoshell" particle. We have both numerically and experimentally studied the optical efficiencies of titania (TiO_2) nucleated in various degrees on silica (SiO_2) nanospheres. We show that optimal surface nucleation over cores of appropriate sizes and optical properties will have a direct impact on the applications exploiting the absorption and scattering properties of such composite particles. © 2013 Optical Society of America

OCIS codes: (160.4760) Optical properties; (160.4236) Nanomaterials; (290.5850) Scattering, particles; (310.6188) Spectral properties; (330.1690) Color.

http://dx.doi.org/10.1364/OL.38.003275

Core-shell composite nanoparticles are significant for their use in photothermal cancer therapy [1], photocatalysis [2–4], cosmetics [5], and specialized optical materials [6–8]. In addition to the well-known applications of nanoparticles in heat assisted killing of cancerous cells, nanostructures can be engineered for heat assisted magnetic recording as well [9]. In the classical limit, when the particle size is greater than 10 nm, the absorbed radiation can be assumed to cause Joule heating. It has been shown that metallic nanostructures can efficiently couple the thermal energy and incident photon to catalytically drive chemical reactions, even at temperatures lower than otherwise possible [2]. Also, targeted drug delivery is a very efficient means to fight cancer [10], and one of the most viable ways to achieve it includes release of the drug by a light trigger [11].

We have studied the absorption and scattering of light in UV and visible regions by composite nanoparticles with inhomogeneous surface coverage on a spherical core. Smaller nanoparticles have larger surface-to-volume ratios and the associated potential benefits in their thermal and catalytic properties, but they pose either health hazards or challenges in stabilization at the required environments, resulting in loss of the desired functional attributes [12–14]. Composite particles with larger cores and surface nucleated smaller nanoparticles are solutions in maintaining a large effective area and increasing the functionality of the surface particles—in addition to increasing their optical efficiency. Different core-shell size ratios allow tuning of optical resonances, and this alone has been the dominant motivation in their widespread application [15–17]. But the effective surface area of a core with a partially nucleated surface can be significantly larger than that of a core-shell particle of the same dimensions, thus increasing its absorption efficiency, and possibly its photocatalytic properties. But, unlike with homogeneous particles, extinction measurements alone do not provide an estimate of the trends in absorption by such composite particles. This is due to the scattering and absorption that can be relatively exclusive in their behavior as a function of surface coverage. Such partial nanoshells have been studied before from a synthesis perspective [18,19], and the additional plasmon resonances due to coupling between the metal clusters of the shell were elucidated using their extinction efficiencies [20–22]. While absorption is the primary consideration in photocatalysis and photothermal applications, both absorption in the UV range and scattering in the visible spectrum have become important in other applications such as biomaterials and cosmetics. Here we study the absorption efficiency of such particles with varying surface coverage, which indeed manifest differently from scattering efficiency alone or the total efficiency of extinction. The composite particles used in our experiments were synthesized by nucleating titania over silica nanoparticles with varying coverage of the surface area. The silica particles are well understood as dielectric spheres, and titania has strong absorption bands in the UV spectrum, making it an ideal absorber of optical radiation; moreover titania synthesis and crystallization have become increasingly environmentally friendly by use of biomimetic templates [23]. Our experimental measurements of extinction along with the numerical results suggest that the absorption of light can be nonmonotonic with increasing area of surface coverage. This effect can be seen as a shift of the mode composition of the composite particle toward higher-order surface modes of a sphere and back toward the dominant dipolar mode in the complete shell particle. Alternately, the properties of such particles can also be elucidated as a result of the strong interaction between the particles on the surface of the core [20,22]. We have numerically studied the absorption and scattering spectra of such particles with varying core sizes and surface coverage, exploring a larger parametric space that is not readily feasible in experiments. Also, decomposition of extinction spectra into its scattering and absorption components for such particles is nontrivial using experiments, while it is relatively straightforward in numerical studies. These results show that they can be tuned to

applications using optimal core sizes and surface fractions.

We used discrete dipole approximations [24] to model the absorption and scattering efficiencies of such composite nanoparticles. In this formulation, the target volume is represented by a lattice of polarizable dipole grains that interact in the presence of the incident field, resulting in net scattering and absorption by the target. Dipole polarizability is computed from the refractive index of the material using the lattice-dispersion Relation [25]. The permittivity of silica as a function of wavelength was obtained from well-known fits of past measurements [26]. The dispersive permittivity of titania nanocrystals in anatase phase used here can be obtained from reflection measurements of thin films [27]; the permittivity of anatase is indeed different from rutile or amorphous forms of titania [28]. A spherical lattice of dipoles (each 15 nm in diameter) represented a silica core randomly populated with titania particles of different fractions on the surface: 0.1, 0.25, 0.5, 0.8, 1, and 2 by area (1 represents the case of a silica core completely covered by titania with a monolayer, and 2 represents coverage with two layers). The numerical results are averaged over many random locations of the titania particles on the core particle, and the cumulative efficiency varies by less than 5% from the average for the spectra (largest deviations observed for lowest surface fraction as expected). The optical efficiencies (Q) are given by the corresponding cross sections (rate of energy flow/intensity of incident energy) normalized by the geometrical area of cross section of the particle:

$$
\begin{aligned}
Q_{\text{scat}} &= \frac{1}{2I_i(\pi a^2)} \int \mathbf{n}\cdot\Re(\mathbf{E}_s \times \mathbf{H}_s^*)\mathrm{d}A, \\
Q_{\text{ext}} &= \frac{1}{2I_i(\pi a^2)} \int \mathbf{n}\cdot\Re(\mathbf{E}_s \times \mathbf{H}_i^* + \mathbf{E}_i \times \mathbf{H}_s^*)\mathrm{d}A, \\
Q_{\text{abs}} &= Q_{\text{ext}} - Q_{\text{scat}}, \qquad (1)
\end{aligned}
$$

where **E** and **H** are the electric and magnetic components of the incident/scattered fields. I_i, a, and **n** are, respectively, the incident intensity, the effective radius of the particle, and the normal to a surface of integration enclosing the particle.

Silica nanoparticles were prepared following the classical Strober's solgel synthesis method [29], using tetra orthosilicate (ex. Aldrich). Titania coated silica were prepared (Fig. 1) using synthesized silica nanoparticles dispersed well in ethanol followed by nucleation of titanium dioxide using titanium (IV) butoxide (ex. Aldrich) as a precursor. Different fractions of surface titania were obtained using aliquots of titanium (IV) butoxide of various concentrations (11.4, 5.7, and 2.9 mmol) with the silica nanospheres. Synthesized particles were washed twice in ethanol and calcined at 700°C for 5 h in a muffle furnace (Thermolyn 48000). Other chemicals

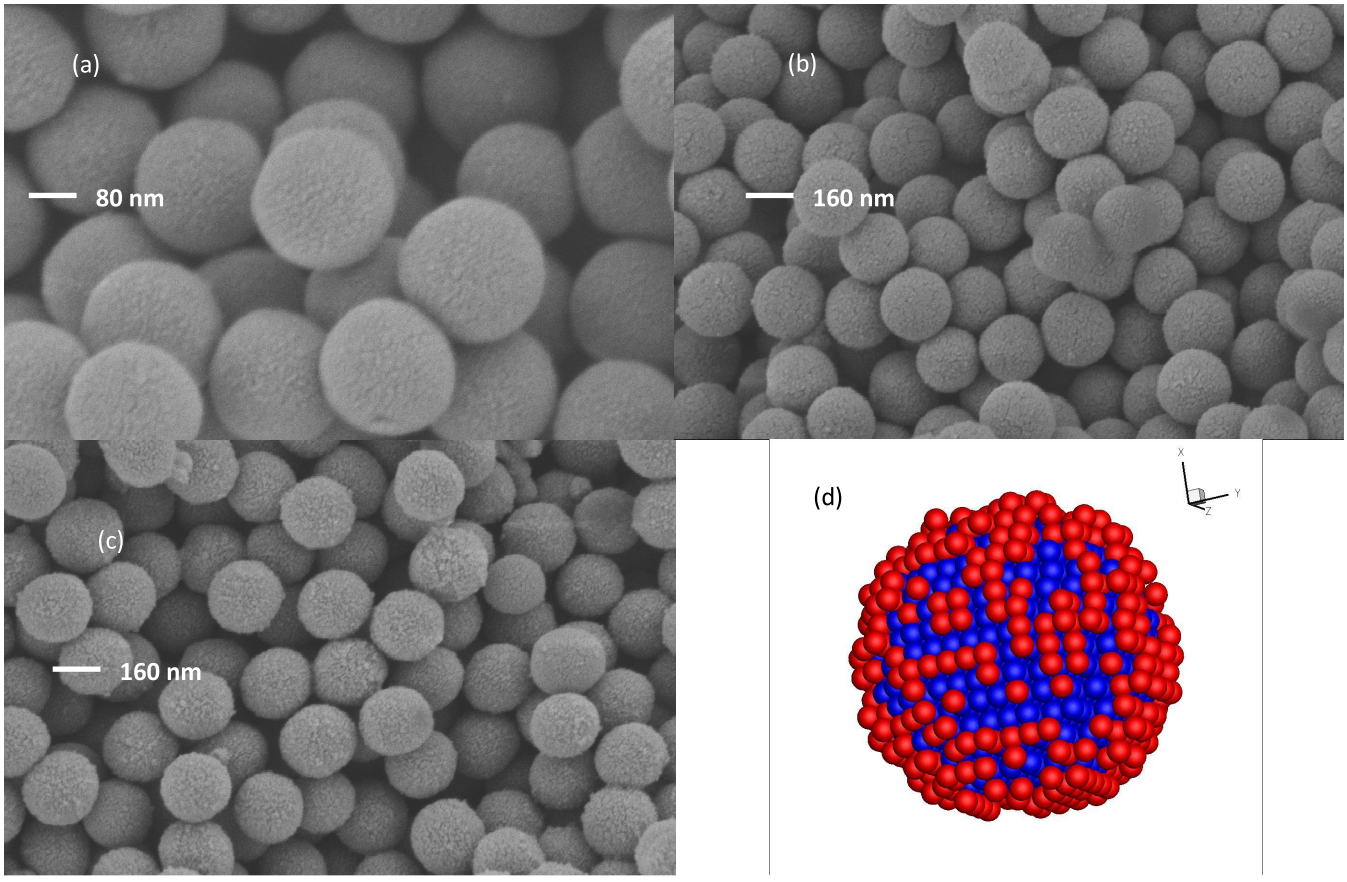

Fig. 1. Scanning electron micrographs of particles synthesized: (a) silica nanospheres, (b) ~0.25 surface fraction of titania, (c) ~0.5 surface fraction of titania, and (d) graphic of the numerically modeled particle with 0.5 surface fraction of titania (surface titania particles in red).

used in the synthesis were ammonia solution (25%) from Merck and spectroscopy grade ethanol from Les Alcohol De Commerce. Additional details of this process have been described elsewhere [5]. The absorption and scattering efficiencies of these composite particles made by nucleating silica spheres (~240 nm diameter) with titania particles of average dimensions ~15 nm were studied. Synthesized particles were dispersed well in ethanol at a dilute concentration of 0.025% assisted by a 30 min sonication. The extinction efficiency of these particles was measured using a dual beam UV–VIS-NIR spectrophotometer (Lamda 900, Perkin Elmer, Inc.) using a quartz cuvette with 10 mm path length.

The experimental measurements of extinction are shown along with the corresponding numerical simulations in Fig. 2(a). The average absorption and scattering spectra of the numerical models are shown in Figs. 2(b) and 2(c). The absorption efficiency increases from ~0.2 for an isolated titania particle to numbers greater than 1 for the composite particle. An optical efficiency of greater than 1 should not be surprising, as a particle can interact with incident light in an area larger than its geometrical cross section; such high efficiencies are typical for particles with dimensions on the order of wavelength. One should also note that the increased absorption by the particles with a surface coverage factor of 0.8 [Fig. 2(b)] compared to a fully covered core-shell particle at certain energies is not anomalous, even if it is counterintuitive. The scattering spectra also exhibit nonlinearity with surface coverage in this range of high absorption and the Mie scattering regime. Nevertheless, the scattering efficiency beyond the spectrum of significant absorption by titania, at larger wavelengths, matches that of a typical Rayleigh scattering homogeneous particle.

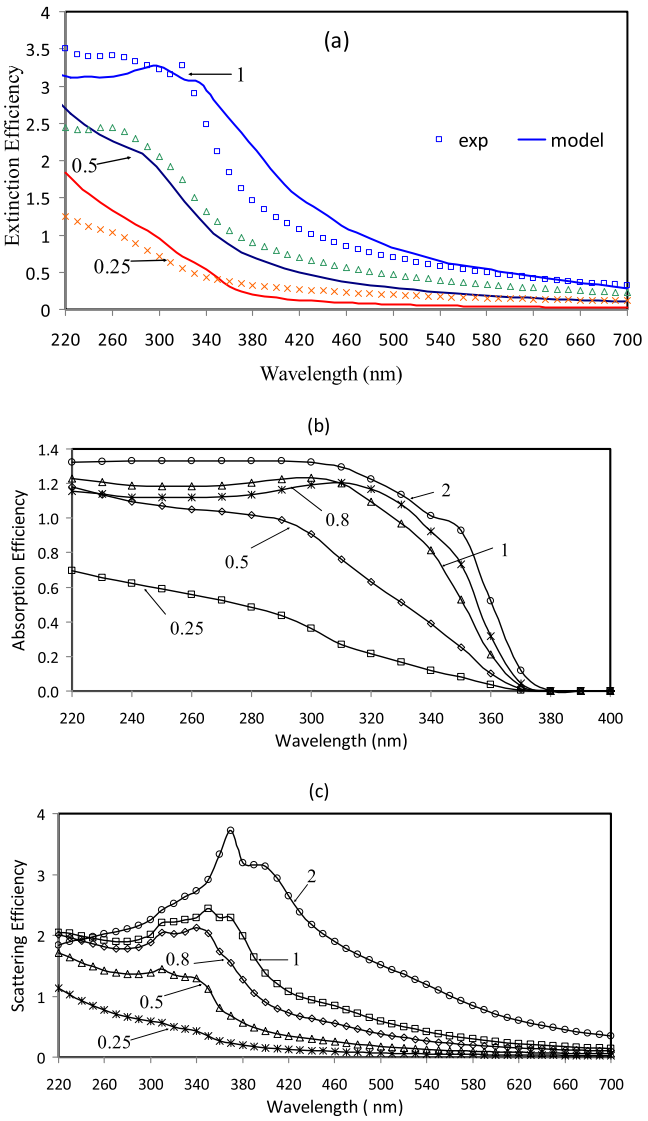

Fig. 2. Nominal surface area fractions of titania and corresponding optical spectra; "2" represents two monolayers of titania particles on the surface. (a) Comparison of the measurements of extinction with numerical models of a nominal composite particle. (b) Computed absorption spectra for various surface fractions of nucleation. (c) Computed scattering spectra of the same composite particles.

Results in Fig. 3(a) show the signs of saturation in absorption efficiency with the increase of titania nucleation on the surface, but an approximately linear increase in the scattering spectra for the most part. The relative volume efficiency of absorption in particular [plotted in Fig. 3(b)] is significant as well. The volume efficiency of absorption (energy density in the material) is given

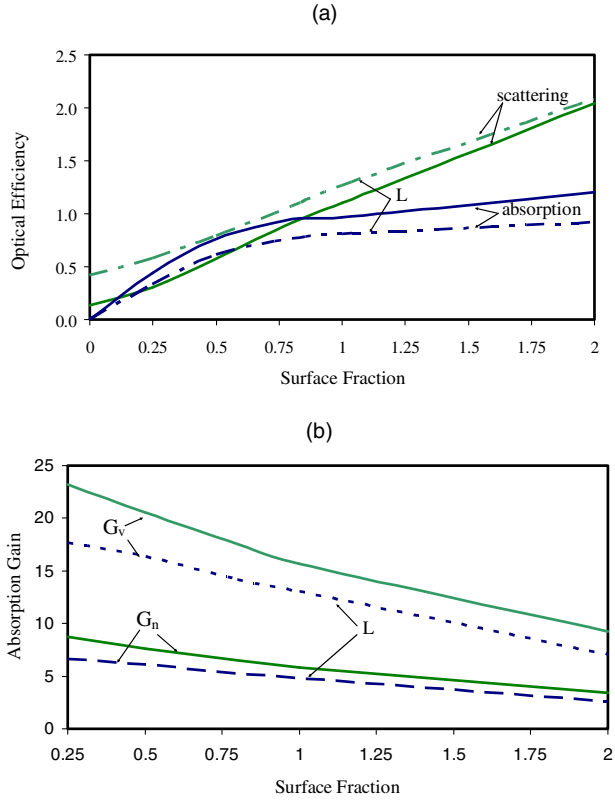

Fig. 3. "L" represents numerical results for a silica core 480 nm in diameter that is larger than the 240 nm silica spheres used in the experiments. (a) Average UV (200–360 nm wavelength) absorption and UV–VIS (200–700 nm wavelength) scattering efficiencies of silica particle with varying surface fractions of titania. (b) UV absorption gain of titania due to silica core. (G_n, absorption of composite particle normalized by the sum absorption of an identical number of isolated titania particles; G_v, absorption of composite particle normalized by absorption of a homogeneous titania sphere that is volume equivalent with total surface nucleation.)

by the absorption cross section normalized by the volume rather than the area of the cross section of the particle [as in Eq. (1)]. A homogeneous nanosphere significantly smaller than the wavelength will have an absorbed energy increase in proportion to its volume ($\sim ka^3$, where "a" is its radius and "k" is the magnitude of the incident wave vector), and thus the absorbed energy density is nearly a constant with increase in size. For the larger composite particle, the volume efficiency of absorption significantly changes as a function of the core size and the surface fraction. Further, it is useful to scale the total absorption of the composite particle into a relative volume efficiency of absorption by titania (neglecting the dielectric core). The absorption of titania in the composite particle when normalized by the sum absorption of an identical number of isolated titania particles gives us the gain (G_n) due to the silica core. Absorption of the composite particle normalized by absorption of a homogeneous titania sphere that is volume equivalent with total surface nucleation gives us another estimate (G_v) of the gain due to the silica core. The core does provide a gain in absorption as mentioned before, but its decrease with the surface fraction in Fig. 3(b) should be noted.

These additional numerical studies also show that the size of silica spheres affects the absorption efficiencies noticeably. As the core particles become larger, the scattering efficiency increases as expected in the upper Rayleigh/lower Mie regime, but absorption efficiency of the composite particle saturates as shown in Fig. 3(a). In fact, the smaller core-shell structure allows an absorption efficiency that is greater than its scattering efficiency when the surface fractions are less than 0.8; this is not true for the larger core. This can be explained by the fact that the effective imaginary part of the refractive index of titania is reduced by a factor proportional to the size of the core and its index [30]. On the other hand, reducing the core sizes comparable to the size of the nucleations is not helpful either. In such cases, the increase of surface nucleations of titania can result in saturation of absorption even at lower surface fractions on the core particle.

Our results show that the surface area coverage of incomplete core-shell nanoparticles significantly affects the efficiency of absorption of light. Though the core provides significant gains in extinction efficiency, effects of saturation limit the absorption efficiency in particular. We note that the volume efficiency of absorption in fact reduces with increasing surface nucleation on the core particle. We observe that sufficient control of surface nucleation to control optical properties is indeed possible; the numerical results of extinction by a nominal composite particle match the measurements, notwithstanding possible dispersion of surface coverage in the prepared sample. Thus incomplete nanoshell particles provide a means of efficient photoabsorption. This optimal use of materials for photoabsorption is significant for both functionality of materials/devices and enhanced safety in biomedical applications.

The scanning electron micrographs were obtained at the Center for Nano Science and Engineering at the Indian Institute of Science, Bangalore. We thank Girish Kunte and Varadharaja Perumal for their support in the imaging.

References

1. S. Lal, S. E. Clare, and N. J. Halas, Acc. Chem. Res. **41**, 1842 (2008).
2. P. Christopher, H. Xin, and S. Linic, Nat. Chem. **3**, 467 (2011).
3. M. Murdoch, G. I. N. Waterhouse, M. A. Nadeem, J. B. Metson, M. A. Keane, R. F. Howe, J. Llorca, and H. Idriss, Nat. Chem. **3**, 489 (2011).
4. D. B. Ingram, P. Christopher, and S. Linic, Nat. Mater. **10**, 911 (2011).
5. S. G. Dastidar, P. Bharath, and A. Roy, Bull. Mater. Sci. **34**, 199 (2011).
6. C. Graf and A. van Blaaderen, Langmuir **18**, 524 (2002).
7. H. Ow, D. R. Larson, M. Srivastava, B. A. Baird, W. W. Webb, and U. Wiesner, Nano Lett. **5**, 113 (2005).
8. F. Wang, R. Deng, J. Wang, Q. Wang, Y. Han, H. Zhu, X. Chen, and X. Liu, Nat. Mater. **10**, 968 (2011).
9. R. E. Rottmayer, G. Ju, Y. Hsia, and M. F. Erden, Proc. IEEE **96**, 1810 (2008).
10. J. Hrkach, D. Von Hoff, M. M. Ali, E. Andrianova, J. Auer, T. Campbell, D. De Witt, M. Figa, M. Figueiredo, A. Horhota, S. Low, K. McDonnell, E. Peeke, B. Retnarajan, A. Sabnis, E. Schnipper, J. J. Song, Y. H. Song, J. Summa, D. Tompsett, G. Troiano, T. Van Geen Hoven, J. Wright, P. Lo Russo, P. W. Kantoff, N. H. Bander, C. Sweeney, O. C. Farokhzad, R. Langer, and S. Zale, Sci. Transl. Med. **4**, 128ra39 (2012).
11. S. M. Lubin, W. Zhou, A. J. Hryn, M. D. Huntington, and T. W. Odom, ACS Nano **6**, 3318 (2012).
12. S. A. Mackowiak, A. Schmidt, V. Weiss, C. Argyo, C. von Schirnding, T. Bein, and C. Bräuchle, Nano Lett. **13**, 2576 (2013).
13. K. J. Lee, L. M. Browning, P. D. Nallathamby, T. Desai, P. K. Cherukuri, and X. N. Xu, Chem. Res. Toxicol. **25**, 1029 (2012).
14. Y. Wei, S. Han, J. Kim, S. Soh, and B. A. Grzybowski, J. Am. Chem. Soc. **132**, 11018 (2010).
15. P. K. Jain and M. A. El-Sayed, J. Phys. Chem. C **111**, 17451 (2007).
16. L. Chuntonov, M. Bar-Sadan, L. Houben, and G. Haran, Nano Lett. **12**, 145 (2012).
17. P. Tuersun and X. Han, Appl. Opt. **52**, 1325 (2013).
18. S. L. Westcott, S. J. Oldenburg, T. R. Lee, and N. J. Halas, Langmuir **14**, 5396 (1998).
19. S. L. Westcott and N. J. Halas, Chem. Phys. Lett. **356**, 207 (2002).
20. O. Pena-Rodríguez and U. Pal, J. Phys. Chem. C **115**, 22271 (2011).
21. T. C. Preston and R. Signorell, ACS Nano **3**, 3696 (2009).
22. K. E. Peceros, X. Xu, S. R. Bulcock, and M. B. Cortie, J. Phys. Chem. B **109**, 21516 (2005).
23. S. Bao, C. Lei, M. Xu, C. Cai, and D. Jia, Nanotechnology **23**, 205601 (2012).
24. B. T. Draine and P. J. Flatau, J. Opt. Soc. Am. A **11**, 1491 (1994).
25. B. T. Draine and J. Goodman, Astrophys. J. **405**, 685 (1993).
26. E. D. Palik, *Handbook of Optical Constants of Solids* (Academic, 1985).
27. D. Mergel, D. Buschendorf, S. Eggert, R. Grammes, and B. Samset, Thin Solid Films **371**, 218 (2000).
28. S. Y. Kim, Appl. Opt. **35**, 6703 (1996).
29. W. Stober, A. Fink, and E. Bohn, J. Colloid Interface Sci. **26**, 62 (1968).
30. C. F. Bohren and D. R. Huffman, *Absorption and Scattering of Light by Small Particles* (Wiley-Interscience, 1983).